

**Screen-printable and stretchable hard magnetic ink
formulated from barium hexaferrite nanoparticles**

Journal:	<i>Journal of Materials Chemistry C</i>
Manuscript ID	TC-ART-05-2020-002234.R1
Article Type:	Paper
Date Submitted by the Author:	16-Jul-2020
Complete List of Authors:	Smith, Connor; University of Florida, Electrical and Computer Engineering Sondhi, Kartik; University of Florida, Electrical and Computer Engineering Mills, Sara; University of Florida, Materials Science & Engineering Andrew, Jennifer; University of Florida, Materials Science & Engineering Fan, Z.; University of Florida, Mechanical and Aerospace Engineering Nishida, Toshikazu; University of Florida, Electrical and Computer Engineering Arnold, David; University of Florida, Electrical and Computer Engineering

Screen-printable and stretchable hard magnetic ink formulated from barium hexaferrite nanoparticles

Connor S. Smith^{1*}, Kartik Sondhi¹, Sara C. Mills², Jennifer S. Andrew², Z. Hugh Fan³, Toshikazu Nishida¹, and David P. Arnold¹

¹ Department of Electrical and Computer Engineering, Gainesville, FL 32611, USA

² Department of Material Science and Engineering, Gainesville, FL 32611, USA

³ Department of Mechanical and Aerospace Engineering, Gainesville, FL 32611, USA

E-mail: connor.smith@ufl.edu

Received xxxxxx

Accepted for publication xxxxxx

Published xxxxxx

Abstract

Stretchable electronics have seen an increase in interest for applications in medicine, sensing, and robotics. Current stretchable materials are either intrinsically stretchable, are patterned into stretchable architectures, or are made by forming a composite of some stretchable material and a rigid material with some desired property, such as high conductivity. However, there is a lack of stretchable magnetic materials available in the literature, and devices that combine stretchability and magnetics are limited to using serial fabrication processes such as embedding millimeter scale pieces of magnet into polymer matrices. In this work, a stretchable composite hard magnetic ink made by mixing barium hexaferrite nanoparticles with 9510 One-Part Epoxy Potting Compound and di(propylene glycol) methyl ether is presented. Using screen printing methods, the ink is then used to fabricate a magnetic strain sensor, which acts as a proof-of-concept for the material and process. Results indicate that a stretchable hard magnetic ink can be made that provides a remnant magnetization of 20 kA/m from the barium hexaferrite particle inclusions, as well as a stretchability of at least 100% strain from the epoxy.

Keywords: stretchable materials, stretchable sensors, flexible materials, screen-printing, magnetic nanoparticle composites

1. Introduction

Stretchable electronics have gained increased interest in recent years alongside applications such as wearable electronics, medical monitoring, and soft robotics [1-4]. Generally, stretchable electronic materials can be separated into two groups—intrinsically stretchable materials and stretchable composites [5]. Intrinsically stretchable electronic materials utilize the inherent stretchability found within the bonds of these materials [6-8]. Unfortunately, devices made from intrinsically stretchable materials often suffer from issues including poor electrical performance and limited stretchability. In comparison, stretchable composites are realized in one of two ways, 1) by patterning a usually rigid material in such a way that it can withstand greater strain than

usual, or 2) from mixing a relatively rigid material with some desired property (such as a high conductivity) throughout a highly stretchable matrix material. Serpentine and ribbon-like structures are common examples of the first of these two types of stretchable composites, but these only allow for limited designs and can require complex fabrication methods [9-11]. The second type of stretchable composites are often simpler to produce, as they only involve combining ingredients such as nanoparticles or flakes with a stretchable material to form composites with combined properties. Further, by lowering the viscosity of these mixtures, these composite materials can be formed into inks that can be deposited with screen-printing, which is a proven batch-manufacturing technique with great promise in the area of stretchable electronics [12-14]. An example of a screen printable composite material includes conductive silver ink made from silver flakes and epoxy which

has been used to make stretchable and flexible coils, antennas, and sensors [15-18].

While many types of stretchable composite inks are currently available, there is not a wide variety of stretchable composite magnetic inks. Such magnetic inks would be formed by mixing magnetic nanoparticles with a stretchable polymer and solvent and then screen-printed and patterned into a variety of features. The result is a stretchable and screen-printable magnetic material that can fill gaps in current stretchable electronic technologies including stretchable sensors, stretchable power electronics, and micro-robotics. Currently, magnetic materials are often included in stretchable devices by embedding millimeter scale magnets cut from larger bulk magnets into a stretchable matrix made from materials such as PDMS [19-24]. However, this method is a serial process and involves individually cutting and placing magnets in a specific pattern before surrounding them with the stretchable matrix material. In contrast, a stretchable composite magnetic ink made from magnetic nanoparticles and a polymer would allow for the batch fabrication of stretchable magnetic devices using screen-printing. In this work, a stretchable hard magnetic ink made from a mixture of barium hexaferrite nanoparticles and commercially purchased epoxy is presented and characterized. The ink is then used to fabricate a magnetic strain sensor that is based on previous designs from *Zhang et al.* as a proof of concept for the material [19]. This will demonstrate the potential applications for the magnetic ink in this work and promote the development of other types of magnetic ink and their applications.

2. Materials and Methods

2.1 Magnetic Ink

The stretchable magnetic ink is formed by mixing barium hexaferrite nanoparticles from Nanostructured & Amorphous Materials, Inc. located in Katy, Texas, U.S.A. (average diameter of 500 nm) with 9510 One-Part Epoxy Potting Compound (epoxy) from MG Chemicals and di(propylene glycol) methyl ether (DPGME) from Acros Organics. Table 1 shows the mass ratios used throughout this work. This composition ratio was chosen so that the final weight percentage of barium hexaferrite in the cured ink would be 80% to maximize the amount of magnetic material present. Note that the value of 80% is calculated by dividing the mass ratio of the barium hexaferrite nanoparticles by the combined mass ratios of the nanoparticles and the epoxy, as the DPGME is expected to be completely removed during curing. The mass ratio of DPGME used comes from the need for the ink to still be fluid enough to be screen-printed in its un-cured form. The mass ratio of 30% DPGME was determined through trial and error, where smaller mass ratios of DPGME led to inks that were too viscous for screen-printing. Mass ratios of DPGME above what was required for screen-printing were not

desirable either since the DPGME is removed during curing and so excess solvent would be wasted. Further, excess solvent would likely lead to shrinking and voids in the cured film and, if too much solvent is added, can interfere with the quality of the screen-printing as the ink would begin spreading on the substrate after passing through the screen.

TABLE I
Recipe for Magnetic Ink

Ingredient	Mass Ratio
barium hexaferrite nanoparticles	56%
9510 epoxy potting compound	14%
di(propylene glycol) methyl ether	30%

First, barium hexaferrite nanoparticles were placed into a plastic weigh boat and their mass was measured on an analytical balance. The epoxy and DPGME were then added to this weigh boat and mixed using a metal spatula for one minute until a homogenous mixture was formed. Samples were cured in a Lindberg/Blue M oven at 120°C for 10 minutes. Multiple tests were performed to characterize the mechanical, material, and magnetic properties of the magnetic ink. The Young's moduli of the printed magnetic ink was calculated using the micro-indentation method. This method has been described elaborately in Feng et al. [25]. This method uses a conical indentation tip and this tip is controlled by a motor and a program developed specifically for a Mark-10 Test Stand (model no.: ESM303). The tip applies a force on the material of interest, this force is also measured using the Mark-10. The force and indentation depth are used to calculate the Young's modulus of the material. Images of the surface of a cured sample of the magnetic ink were performed using a FEI Nova 430 SEM. Images of the surface of a dried film of barium hexaferrite nanoparticles were also collected for comparison. Samples were analyzed via X-ray powder diffraction patterns using a Panalytical X'pert powder diffractometer with a Cu anode ($K\alpha$ radiation, $\lambda = 1.54 \text{ \AA}$) and scintillation detector (45 kV, 40 mA). The barium hexaferrite ($\text{BaFe}_{12}\text{O}_{19}$) nanopowder and magnetic ink samples were scanned with a step size of 0.008° . The phase of barium hexaferrite was then confirmed in both the powder and composite with comparison to reference pattern 00-007-0276 for barium hexaferrite from the International Center for Diffraction Data (ICDD). For magnetic characterization, the ink was printed as a 1 cm^2 square onto a TPU substrate and characterized using an ADE Tech. EV-9 VSM with max fields of 1800 kA/m to measure and plot its hysteresis curve. Thermogravimetric analysis (TGA) was performed on the magnetic ink in order to determine the decomposition point of the epoxy. Approximately 1.8 mg of the magnetic ink sample was placed in a 100 μL platinum pan and loaded into a TA

Instruments Q5000 thermogravimetric analyzer. The sample was heated, under a continuous nitrogen purge, at 5°C/min to 100°C and held at 100°C for 10 minutes. Heating then continued at 5°C/min to 500°C, with a hold at 500°C for 10 minutes.

3.1 Proof of Concept Magnetic Strain Sensors

As a proof of concept for the magnetic ink, a set of magnetic strain sensors, replicated from those designed by *Zhang et al.*, were fabricated and characterized [19]. Figure 1 shows the process flow used to fabricate the magnetic strain sensors. First, following the recipe and method described above, the magnetic ink was made from mixing the barium hexaferrite particles, epoxy, and DPGME. Then, using a mask made from a 76 µm thick sheet of cyclic olefin co-polymer (COC) patterned using a Graphtec Craft ROBO Pro (model no.: CE5000-40-CRP), the device patterns were screen-printed onto a thermal polyurethane (TPU) substrate with a stiff plastic backing to form ~100 µm thick features. After curing the devices at 120°C for 10 minutes, a ~50 µm thick layer of polydimethylsiloxane (PDMS) was screen-printed on top of the magnetic portions of the device to act as a protective encasement, and then this layer was cured at 75°C for about 1 hour. Finally, the TPU was cut into pieces to form the individual sensors, and the stiff plastic backing on the TPU was removed by hand. An Oersted Technology (Model 340B) pulse magnetizer was then used to magnetize the magnetic sections of the device in the out-of-plane, positive z-direction using a ~1T field.

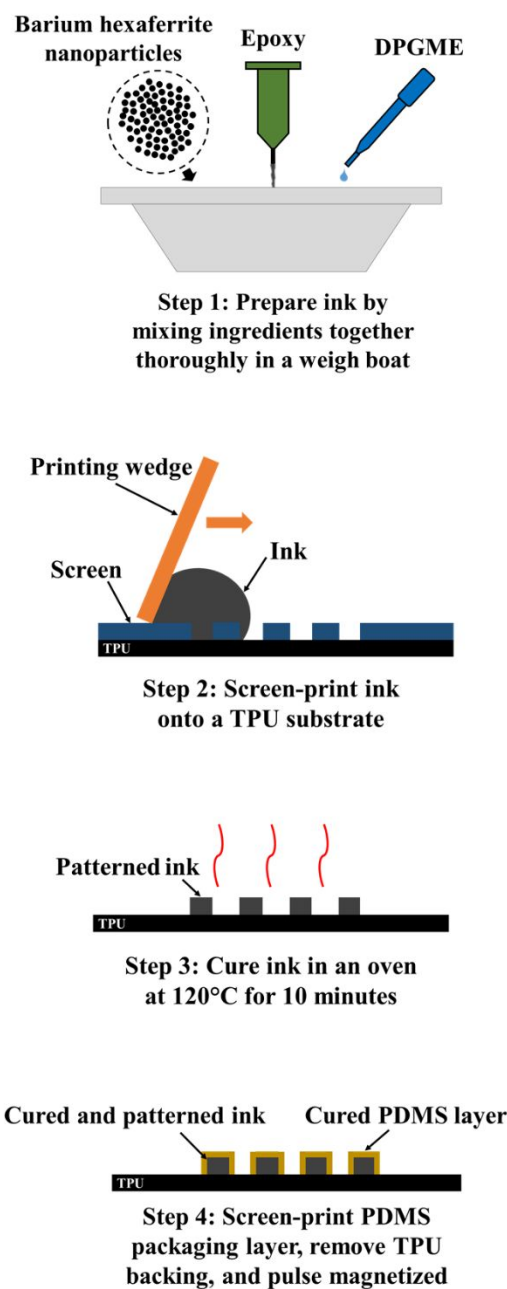


Fig. 1 – Process flow for fabricating magnetic strain sensors. First the barium hexaferrite nanoparticles, epoxy, and DPGME are mixed to form the hard magnetic ink. Then the samples are screen-printed onto a TPU substrate using the doctor blade method. Next the patterned ink is cured in an oven at 120°C for 10 minutes. Finally, a PDMS packaging layer is screen-printed onto the device and the backing of the TPU is peeled off and the final strain sensor with cured ink remains.

Figure 2 shows an illustration of the three differently spaced magnetic strain sensors that were fabricated and tested. The size of the magnetic sections on each of the sensors was

kept the same (3x10 mm) while the spacing between them was changed for each sensor. Figure 2a shows a sensor with a spacing of 4 mm between its magnetic sections, Figure 2b shows a sensor with a spacing of 6 mm, and Figure 2c shows a sensor with a spacing of 8 mm. It is expected that by increasing the spacing between the magnetic sections, the overall field produced by the sensor, and the sensor's sensitivity, should decrease. This decrease in sensitivity is due to a decrease in the magnetic field gradient between the magnetic sections (which are all magnetized in the same out-of-plane, positive z-direction) as they move farther apart.

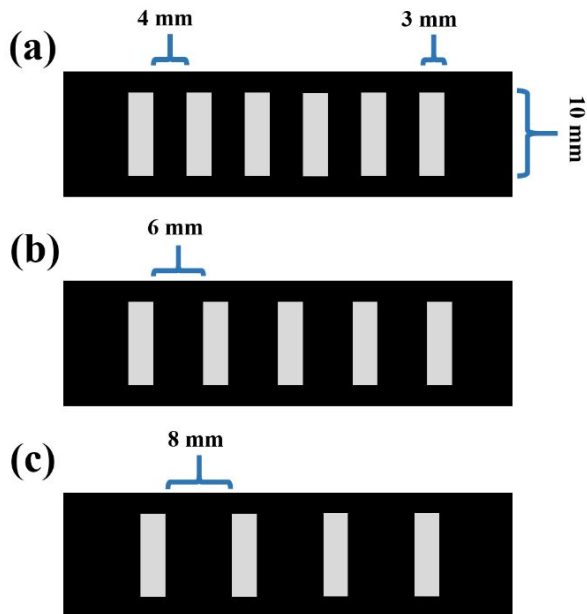


Fig. 2 – Illustration of the three different strain sensors that were fabricated with spacings between magnetic materials of (a) 4 mm, (b) 6 mm, and (c) 8 mm. These designs are the same as seen in Zhang et al. [19].

Figure 3 shows an illustrated mock-up of the test setup used to characterize the magnetic strain sensors. An F.W. Bell Series 9950 Gauss/Teslameter with an F.W. Bell 8000 Series 3-Axis Hall Probe was calibrated and placed into a holding fixture. The probe was placed 1 cm away from the sensors under test. Note that the Hall sensor embedded in the probe is not located directly at the tip, but its location is accounted for in the 1 cm separation. The sensor under test is then strained, and the gaussprobe is used to record the change in the magnetic field produced by the magnetic sections of the device. The percent change in magnetic field versus the percent strain is plotted for each sensor. A linear regression is used to fit the data, and the sensitivity is taken as the slope of the resulting line. A maximum of 100% strain was applied for each device due to physical limitations of the setup. Further, a sensor was cycled between 0% and 30% strain using a Mark-10 Test Stand for 1-500 cycles, and the percent change in the magnetic field produced by the sensors was measured to

understand the change in behavior for the device after multiple cycles.

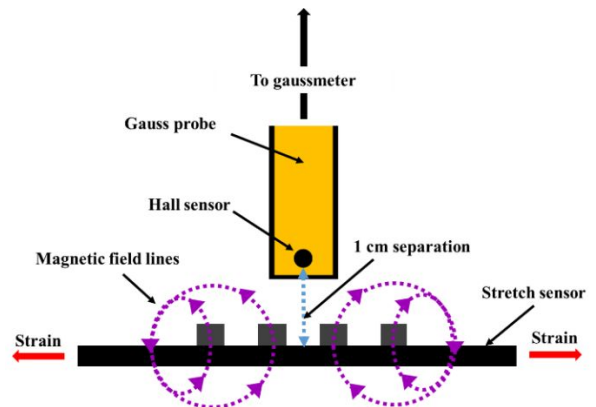


Fig. 3 – Illustration of the test setup used to measure the change in the magnetic field produced by the sensors after being stretched. Note that the Hall sensor in the Gauss probe is not directly at the tip of the probe, so the 1 cm separation between the Hall sensor and the strain sensor includes this distance from the tip.

3. Results and Discussion

3.1 Characterization of Magnetic Ink

The Young's modulus of the material on the TPU substrate was found to be 2.65 ± 0.32 GPa. Figure 4 shows SEM images of the barium hexaferrite particles and cured magnetic ink. Figure 4a shows the top surface of a film of barium hexaferrite particles that were suspended in water, dispensed onto a glass slide, and dried in an oven at 120°C. Figure 4b shows the top surface of a cured magnetic ink film that was screen-printed onto a glass slide and cured in an oven at 120°C. The apparent distribution of barium hexaferrite particles appears unchanged between the two images, with the primary change being the presence of the epoxy binding agent in Figure 4b. Further, these SEM images allow for closer inspection of the barium hexaferrite particles size distribution. A wide distribution of particle sizes is seen in Figure 4a, with the smallest particles appearing to be less than 500 nm in diameter, and the largest being over 1 μm in diameter. However, particles of all sizes exhibit thin hexagonal prism shapes, which is expected due to the crystal structure of the barium hexaferrite [26, 27].

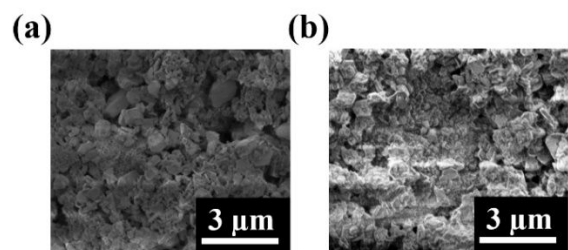


Fig. 4 – SEM images of (a) the barium hexaferrite particles dried onto a glass slide and (b) the magnetic ink (barium hexaferrite particles with the epoxy) printed and cured on a glass slide. Note the charging effects in (b) that arise from the presence of the insulating epoxy in the ink.

Figure 5 shows optical profilometry measurements of the surface of a cured magnetic ink film. From this image, a surface roughness of 2.74 μm was determined. The presence of particles throughout the ink contributes to this surface roughness, as well as the expected loss in volume caused by the removal of solvents during the curing process. This surface roughness is similar to those of other inks, such as the conductive silver inks seen in the study by *Mikkonen et al.* [28]

TABLE 2

Magnetic Parameters from dc Hysteresis Curve

Parameter	Value
Saturation (M_S)	60 kA/m
Remanence (M_r)	20 kA/m
Coercivity (H_c)	50 kA/m
Squareness (M_r/M_S)	0.33

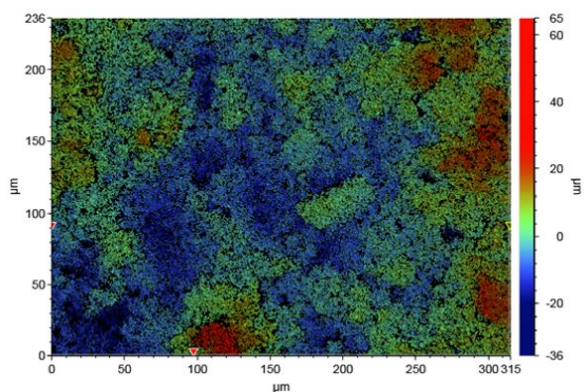


Fig. 5 – Optical profilometry measurement of the surface of a printed and cured magnetic ink sample. Results showed a surface roughness of 2.74 μm .

Figure 6 shows the XRD plots of the barium hexaferrite particles and a cured magnetic ink film. Both the barium hexaferrite nanopowder and corresponding magnetic ink are compared to a reference pattern for hexagonal barium hexaferrite (00-007-0276). The diffraction pattern of the $\text{BaFe}_{12}\text{O}_{19}$ nanopowder, along with that of the magnetic ink, are both composed of hexagonal $\text{BaFe}_{12}\text{O}_{19}$, as expected. The

magnetic ink retains the characteristic peaks of hexagonal $\text{BaFe}_{12}\text{O}_{19}$.

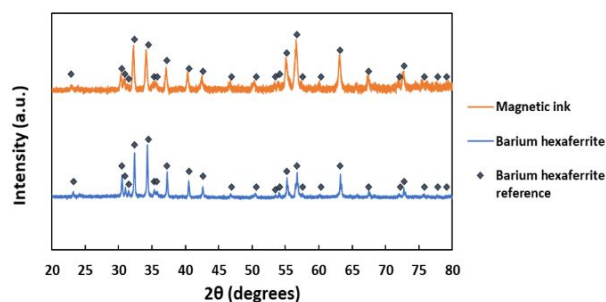


Fig. 6 – XRD plots of the barium hexaferrite nanoparticles (bottom plot) and magnetic ink (top plot). Note that the magnetic ink plot retains the characteristic peaks of hexagonal $\text{BaFe}_{12}\text{O}_{19}$ (reference ID 00-007-0276).

Figure 7 shows a DC VSM hysteresis curve for a film of cured magnetic ink, and Table 2 details the different magnetic parameters determined from this measurement. The magnetic saturation (M_S) is found to be 60 kA/m, the remnant magnetization (M_r) is found to be 20 kA/m, the coercivity (H_c) is found to be 50 kA/m, and the squareness (M_r/M_S) is calculated as 0.33. Notably, a magnetic remanence of 20 kA/m indicates that the cured magnetic ink acts as a permanent magnet due to the inclusion of the hard magnetic particles.

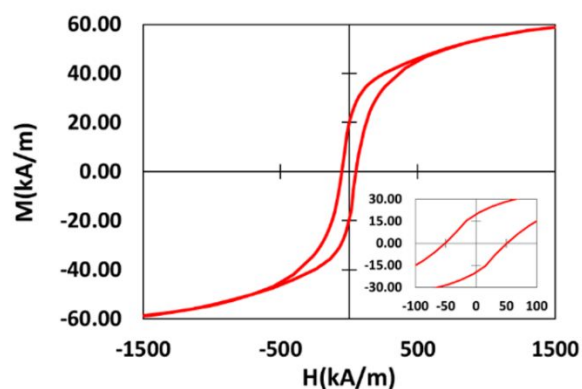


Fig. 7 – DC VSM hysteresis curve for the barium hexaferrite magnetic ink. Note the specific magnetic parameter values given in Table 2. (Inset: zoom-in of the curve to show intercepts.)

Figure 8 shows a TGA plot of a film of uncured magnetic ink. A low temperature drop occurs due to the curing process, while another drop occurs at $\sim 300^\circ\text{C}$. This indicates the point when the epoxy in the ink begins decompose. From this, an upper limit of $\sim 300^\circ\text{C}$ is apparent for the operating temperature of this ink and any devices made from it.

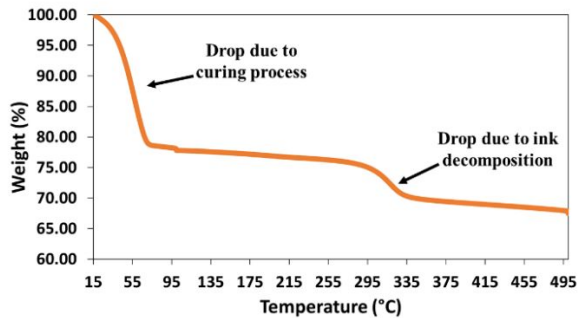


Fig. 8 – TGA plot of the cured magnetic ink. Note that a drop in mass occurs at $\sim 300^{\circ}\text{C}$, indicating the point when the epoxy in the ink begins to break down.

3.2 Characterization of Proof of Concept Magnetic Strain Sensors

Figure 9 shows optical microscopy images of the magnetic strain sensors fabricated using the process seen in Figure 1. The magnetic portions of all the devices were able to be printed in the desired dimensions of 10 mm by 3 mm. Figure 9a shows the device with 4 mm spacing between the magnetic features, Figure 9b shows the device with 6 mm spacing between the magnetic features, and Figure 9c shows the device with 8 mm spacing between the magnetic features. Note that the surface of the devices appears shiny due to the presence of the cured PDMS packaging layer.

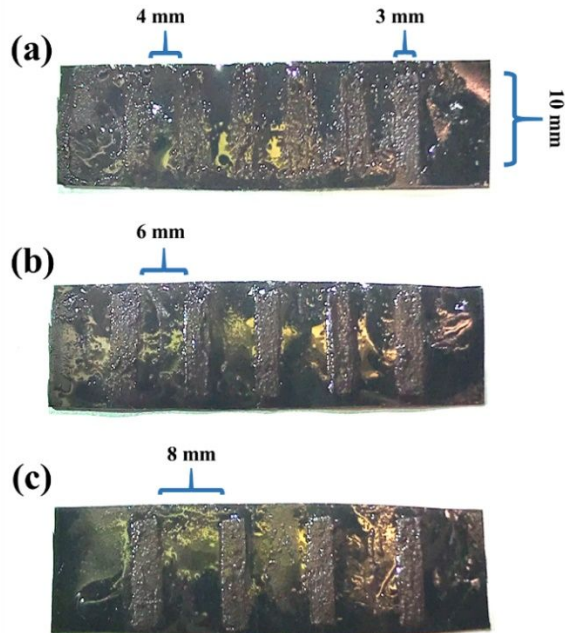


Fig. 9 – Optical image of the three different fabricated strain sensors with spacings between magnetic materials of (a) 4 mm, (b) 6 mm, and (c) 8 mm. Note that the surface appears shiny due to the presence of the cured PDMS packaging layer.

Figure 10 shows the plot of the measured magnetic field above the sensors versus applied strain. Results were collected for the three differently spaced sensor designs, and the sensitivity of each was calculated as the percent change in the measured magnetic field per the percent change in the applied strain. These sensitivities were found to be -0.49, -0.64, and -0.81 for the 8 mm spaced, 6 mm spaced, and 4 mm spaced samples, respectively. From this, an indirect relationship is seen between the spacing between the magnetic portions of the sensor and the sensitivity of the device. A similar trend is noted in the work from Zhang *et al.* [16] where the design of these devices was found. This result is also expected because as the magnetic portions (which are magnetized in the same out-of-plane, positive z-direction) are brought closer together, the magnetic field gradient between them increases. Further, while the samples were only measured up to 100% strain due to physical limitations of the measurement setup, it is notable that the devices could have likely been stretched beyond these limits before breaking. However, further strain is also expected to cause a non-linear response from the sensor, which is not ideal for sensor operation. This result helps to show that the magnetic ink presented in this paper has practical use in making functioning devices.

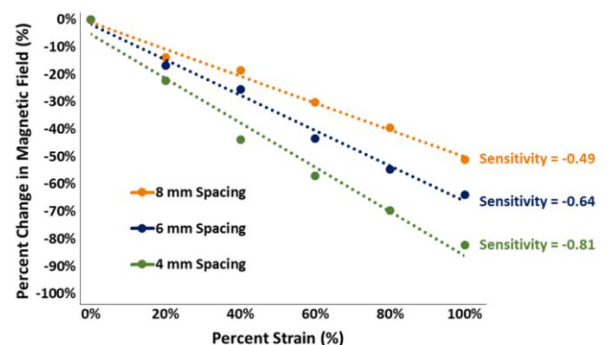


Fig. 10 – Plot of the percent change in magnetic field versus the percent change in strain experienced by each of the differently paced magnetic strain sensors. Note that the sensitivity (slope) of the sensors drop as the spacing between the magnet features increase, which agrees with previously seen results [16].

Figure 11 shows the plot of the percent change of the measured magnetic field versus the number of 30% strain cycles underwent by the sensor. A saturation of the value of the magnetic field occurs between 1 and 10 cycles at a value of $\sim 75\%$. This data shows that devices made from the ink presented in this paper would require at most 10 cycles at a reasonable strain of 30% before proper calibration could occur. This would allow the magnetic field produced by the device to saturate at a constant value that is $\sim 75\%$ the initially measured magnetic field. This saturation is likely to be caused by a shift in the initial location of the field producing magnetic

particles in the ink that would occur during initial stretching. A shift in the location of the particles would cause a change in the measured magnetic field but, once shifted, these particles would be expected to follow a similar pattern during future stretches.

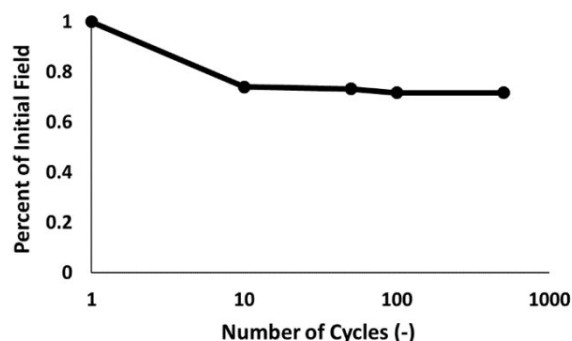


Fig. 11 – Plot of the change in the percent of the initial magnetic field measured versus the number of 30% strain cycles underwent by the sensors. Note that the sensors see a saturation of the measured initial field at about ~75% between 1 and 10 cycles.

4. Conclusion

This work describes the fabrication and characterization of a screen-printable and stretchable hard magnetic ink made using barium hexaferrite nanoparticles. Further, a proof of concept is provided by fabricating and analyzing a magnetic strain sensor made from the hard magnetic ink. Results indicate that the ink can be screen-printed, and results in a surface roughness of just 2.74 μm . SEM, VSM, and XRD results show that the barium hexaferrite particles remain in the printed inks, and that the ink maintains the magnetic properties and characteristic peaks of the particles. Finally, TGA shows that the maximum operating temperature of this ink is $\sim 300^\circ\text{C}$, as that is the point where the epoxy in the ink begins to break down. Using screen-printing, three different strain sensors were made with different spacing between the magnetic portions. These sensors were then stretched and the magnetic field they produced by the magnetic material was measured as a function of strain. Results showed a similar pattern of decreased sensitivity with increased spacing of the magnetic material on the sensors as seen in previous work by Zhang *et al.* [16]. The samples were also cycled with 30% strain up to 500 times in order to see how the field produced by the magnetic material changed after multiple cycles. Results showed that the field produced by the magnetic material saturated at $\sim 75\%$ its initial value between 1 and 10 cycles, indicating how the cured magnetic ink reaches a consistent value once initially cycled. This work looks to increase interest in the design and application of stretchable magnetic inks, and future work will

focus on designing other types of inks (such as a soft magnetic ink) and applying them in sensor, medical, and stretchable electronic devices.

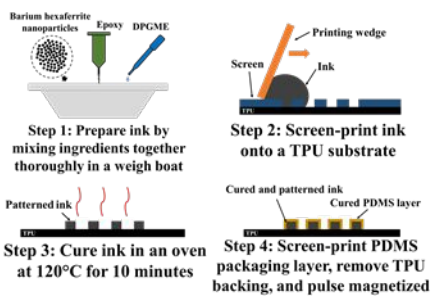
Acknowledgements

This work was supported by the NSF I/UCRC on Multi-functional Integrated System Technology (MIST Center) IIP-1439644. The authors thank the staff of the Herbert Wertheim College of Engineering Research Service Center at the University of Florida for assistance in the material analysis.

References

- [1] Ahn J and Je J 2012 *Journal of Physics D: Applied Physics* **45** 103001
- [2] Kim B and Rogers J 2008 *Advanced Materials* **20** 4887
- [3] Liu Y, Pharr M and Salvatore G 2017 *ACS Nano* **11** 9614
- [4] Lu N and Kim D 2014 *Soft Robotics* **1** 53
- [5] Lipomi D 2016 *Advanced Materials* **28** 4180
- [6] Yu Z, Niu X, Liu Z and Pei Q 2011 *Advanced Materials* **23** 3989
- [7] Liang J, Li L, Chen D, Hajagos T, Ren Z, Chou S, Hu W and Pei Q 2015 *Nature Communications* **6** 1
- [8] Savagatrup S, Printz A, O'Connor T, Zaretski A and Lipomi D 2014 *Chemistry of Materials* **26** 3028
- [9] Lacour P and Wagner S 2004 *Journal of Vacuum Science and Technology A* **22** 1723
- [10] Xu S, Zhang Y, Cho J, Lee J, Huang X, Jia L, Fan J, Su Y, Su J, Zhang H, Cheng H, Lu B, Yu C, Chuang C, Kim T, Song T, Shigetaka K, Kang S, Dagdeviren C, Petrov I, Braun P, Huang Y, Paik U and Rogers J 2012 *Nature Communications* **10** 1
- [11] Zhang Y, Fu H, Su Y and Xu S 2013 *Acta Materialia* **61** 7816
- [12] Rogers J, Someya T and Huang Y 2010 *Science* **327** 1603
- [13] Suikkola J, Björnininen T, Mosallaei M, Kankkunen T, Iso-keitola P, Ukkonen L, Vanhala J and Mäntysalo M, 2016 *Scientific Reports* **6** 1
- [14] Mohammed M and Kramer R 2017 *Advanced Materials* **29** 1604965
- [15] Amontree J, Sondhi K, Hwangbo S, Avuthu S, Yoon Y, Nishida T and Fan Z 2018 *Proceedings of 6th IEEE WiSEE Conference* 119
- [16] Sondhi K, Hwangbo S, Yoon Y, Nishida T and Fan Z 2018 *Journal of Micromechanics and Microengineering* **28** 125014
- [17] Sondhi K, Amontree J, Hwangbo S, Guruva S, Avuthu R, Yoon Y, Fan Z and Nishida T 2018 *Proceedings of IEEE Sensors* 1
- [18] Smith C, Sondhi K, Fan Z, Nishida T and Arnold D 2019 *Proceedings of IFETC 2019*
- [19] Zhang T, Ochoa M, Rahimi R and Ziaie B 2017 *Proceedings of IEEE MEMS 2017* 235.
- [20] Donolato M, Tollan C, Porro J, Berger A and Vavassori P 2013 *Advanced Materials* **25** 623
- [21] Melzer M, Makarov M, Calvimontes A, Karnaushenko D,

- Baunack S, Kaltofen R, Mei Y and Schmidt O 2011 *Nano Letters* **11** 2522
- [22] Lazarus N and Bedair S 2016 *Applied Physics A* **22** 542
- [23] Melzer M, Karnaushenko D, Lin G, Baunack S, Makarov D and Schmidt O 2015 *Advanced Materials* **27** 1333
- [24] Lazarus N, Meyer C, Bedair S, Slipher A and Kierzewski I 2015 *ACS Applied Materials & Interfaces* **7** 10080
- [25] Feng C, Tannenbaum J, Kang B and Alvin M 2010 *Experimental Mechanics* **50** 737
- [26] Townes W, Fang J and Perrotta 1967 *Crystalline Materials* **125** 437
- [27] Goto K, Ito M and Sakurai T 1980 *Japanese Journal of Applied Physics* **19** 1339
- [28] Mikkonen R and Mäntysalo M 2018 *Microelectronics Reliability* **86** 54



Stretchable composite hard magnetic ink made from barium hexaferrite nanoparticles and epoxy is used to fabricate a magnetic strain sensor.